

Magnetic tunnel junctions with monolayer hexagonal boron nitride tunnel barriers

Cite as: Appl. Phys. Lett. **108**, 102404 (2016); <https://doi.org/10.1063/1.4943516>

Submitted: 05 November 2015 . Accepted: 25 February 2016 . Published Online: 08 March 2016

M. Piquemal-Banci, R. Galceran , S. Caneva , M.-B. Martin, R. S. Weatherup, P. R. Kidambi , K. Bouzehouane, S. Xavier, A. Anane, F. Petroff, A. Fert, J. Robertson, S. Hofmann, B. Dlubak, and P. Seneor



View Online



Export Citation



CrossMark

ARTICLES YOU MAY BE INTERESTED IN

[Electron tunneling through atomically flat and ultrathin hexagonal boron nitride](#)

Applied Physics Letters **99**, 243114 (2011); <https://doi.org/10.1063/1.3662043>

[Perspectives for spintronics in 2D materials](#)

APL Materials **4**, 032401 (2016); <https://doi.org/10.1063/1.4941712>

[Protecting nickel with graphene spin-filtering membranes: A single layer is enough](#)

Applied Physics Letters **107**, 012408 (2015); <https://doi.org/10.1063/1.4923401>

Lock-in Amplifiers
up to 600 MHz



Watch



Magnetic tunnel junctions with monolayer hexagonal boron nitride tunnel barriers

M. Piquemal-Banci,¹ R. Galceran,¹ S. Caneva,² M.-B. Martin,² R. S. Weatherup,²
 P. R. Kidambi,² K. Bouzehouane,¹ S. Xavier,³ A. Anane,¹ F. Petroff,¹ A. Fert,¹
 J. Robertson,² S. Hofmann,² B. Dlubak,¹ and P. Seneor¹

¹Unité Mixte de Physique, CNRS, Thales, Univ. Paris-Sud, Université Paris-Saclay, Palaiseau 91767, France

²Department of Engineering, University of Cambridge, Cambridge CB21PZ, United Kingdom

³Thales Research and Technology, 1 avenue Augustin Fresnel, Palaiseau 91767, France

(Received 5 November 2015; accepted 25 February 2016; published online 8 March 2016)

We report on the integration of atomically thin 2D insulating hexagonal boron nitride (h-BN) tunnel barriers into Co/h-BN/Fe magnetic tunnel junctions (MTJs). The h-BN monolayer is directly grown by chemical vapor deposition on Fe. The Conductive Tip Atomic Force Microscopy (CT-AFM) measurements reveal the homogeneity of the tunnel behavior of our h-BN layers. As expected for tunneling, the resistance depends exponentially on the number of h-BN layers. The h-BN monolayer properties are also characterized through integration into complete MTJ devices. A Tunnel Magnetoresistance of up to 6% is observed for a MTJ based on a single atomically thin h-BN layer. © 2016 Author(s). All article content, except where otherwise noted, is licensed under a Creative Commons Attribution 3.0 Unported License. [<http://dx.doi.org/10.1063/1.4943516>]

Spintronics has been at the heart of the data storage revolution with the proliferation of data centers and the advent of big data. A key element of this revolution is the magnetic tunnel junction (MTJ).^{1–3} While intense research has been carried out on MTJs, the most commonly used tunnel barrier materials remain MgO or Al₂O₃. The issue with these metal oxides is that, when thinned down, they may present non-uniform thicknesses, pinholes, and defects which influence the performance of the devices. Hence, they are difficult to control at the monolayer scale while 2D materials, natural monolayers, are now available through the large scale chemical vapor deposition (CVD) growth. One can now think of atomically thin MTJs tunnel barriers based on heterojunctions of 2D materials. Additionally, epitaxial monolayers are grown on various ferromagnets (FMs).^{4–7} Even greater tailoring potential could be achieved after the growth through ferromagnet intercalation,^{8,9} which would allow fine tuning of the 2D material/ferromagnet coupling (e.g., resistance-area product, spin polarization, and anisotropy). In this direction, low resistance area products, strong exchange couplings across the interface, and high magnetoresistance ratios were predicted.^{10,11} The development of 2D materials for MTJs thus appears promising with potential now emerging such as passivation against ferromagnet oxidation and spin filtering.⁶ Among the 2D materials, hexagonal boron nitride (h-BN), an insulating isomorph of graphene, has already been proposed as an embedding layer for lateral graphene devices^{12–14} and as a barrier in van der Waals heterostructures,¹⁵ thanks to its atomically thin and chemically inert nature. Moreover, experimentally, h-BN has already showed tunneling behavior in vertical devices.^{16–18} Hence, as supported by theoretical predictions,^{10,11,19} h-BN appears as a very promising tunnel barrier candidate for MTJs. Its characterization in functional MTJs now appears all the more crucial as h-BN is progressively introduced in lateral spintronic devices to enhance the transport properties. Experimentally, a previous study²⁰ reported results on the

fabrication of MTJs based on transferred h-BN obtained by CVD. However, the measured tunnel magnetoresistance (TMR) effect of 0.3%–0.5%, which corresponds to a tunnel spin polarization P of only 0.05%–0.25% for FM/h-BN interfaces (estimation based on the Jullière's formula²¹), was far from expectations.^{10,11,19} In this case, the efficiency of the MTJs may have been impacted by the quality of the interfaces at play.

In this letter, we report on Co/h-BN/Fe MTJ, where the large area monolayer h-BN tunnel barrier is grown directly by CVD on Fe. We show that the atomically thin directly grown CVD h-BN exhibits tunneling of the spin polarized electrons with a TMR of 6% and spin polarization P of 17%, two orders of magnitude larger than previously reported for complete MTJs incorporating the h-BN tunnel barriers. First, we perform the characterization of the tunnel properties of h-BN on Fe via Conductive Tip Atomic Force Microscopy (CT-AFM) measurements (Figure 1). Then, we focus on the integration of h-BN into complete magnetic tunnel junctions and their characterization (Figures 2 and 3).

The characterization of the tunnel properties of the h-BN layer is shown in Figure 1. Given that monolayer h-BN is a recently discovered material, very few experimental studies have been carried out to evaluate the monolayer h-BN tunnel barrier properties.^{16–18} In our study, the samples consist of Fe (1 μ m thick, 99.99% purity) prepared by sputtering on an oxidized Si wafer (SiO₂ (300 nm)/Si). The growth of h-BN on Fe is carried out by low pressure chemical vapor deposition with an undiluted borazine precursor, as previously reported.⁷ Briefly, pieces of 7 \times 7 mm² are diced and placed in a custom-built, cold-wall reactor (Aixtron Black Magic 3, base pressure 1 \times 10^{–6} mbar). The samples are first annealed in 3.6 mbar of H₂. At \sim 940 °C, the H₂ is removed and borazine, (HBNH)₃, is dosed into the chamber via a leak valve until a pressure of 6 \times 10^{–3} mbar is reached. The samples are exposed to borazine for 5 min. After growth,

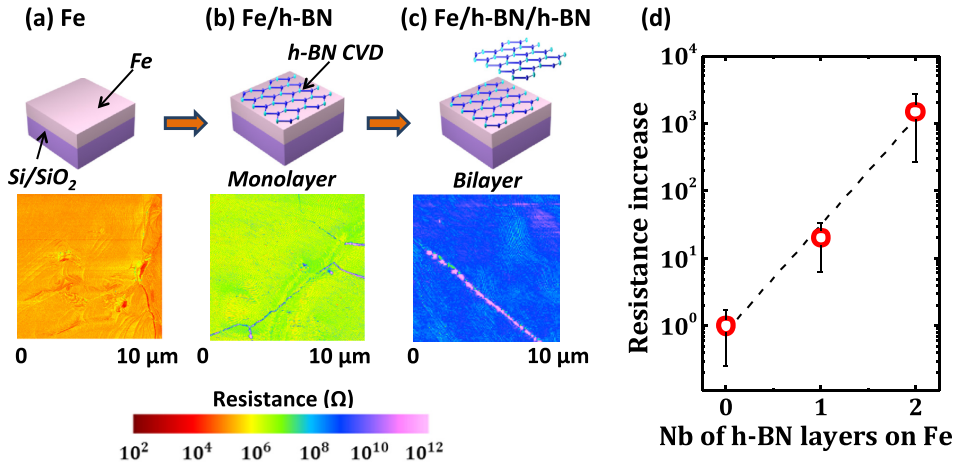


FIG. 1. Resistance CT-AFM mapping of (a) an annealed Fe substrate before h-BN growth, (b) Fe/CVD monolayer h-BN, and (c) Fe/CVD monolayer h-BN with an additional h-BN layer transferred on top (i.e., bilayer h-BN). The measured resistances give approximately $7 \times 10^5 \Omega$ for pristine Fe substrate, $10^7 \Omega$ for Fe/h-BN monolayer, and $10^9 \Omega$ for Fe/h-BN bilayer. (d) Exponential dependence of the resistance normalized against the average resistance of annealed Fe as a function of the number of h-BN layers on Fe ($10^{1.6} \Omega/\text{layer}$ of h-BN).

the borazine is removed, and the heater is switched off. The samples are cooled in vacuum. The characterization of the h-BN layers by the CT-AFM measurements consists of applying a voltage between the substrate and the surface of the sample and measuring the resulting current at the surface. The CT-AFM is thus particularly suited for the characterization of tunnel barriers (thin oxide layers,^{22–24} self-assembled monolayers (SAMs),²⁵ etc.). Here, we measure the tunnel resistance of our samples as a function of the number of h-BN layers. The bias voltage used is 1.5 V. The measurements are made with a highly doped polycrystalline diamond coated tip of 2 N/m at a rate of 0.5 Hz over large scanning areas (tens of microns).

The CT-AFM measurements allow us to extract information about the tunnel behavior of the h-BN and its homogeneity. Figure 1(a) shows a resistance mapping image of an annealed Fe surface before h-BN CVD growth which we use as a baseline. We note that the sample was annealed at the same temperature as that required for the h-BN growth. Figure 1(b) illustrates the resistance mapping image of the Fe surface after CVD growth, thus with monolayer coverage and Figure 1(c) with an additional layer of h-BN, transferred in the same way as reported previously.²⁶ Hence, we have been able to obtain average values of the resistance of the annealed Fe surface before the CVD growth of h-BN, after the growth of h-BN (monolayer) and after the transfer of an additional layer of h-BN (bilayer). The contact resistance values measured between the conductive tip and the surface are approximately $7 \times 10^5 \Omega$ for annealed Fe, $10^7 \Omega$ for Fe/h-BN monolayer, and $10^9 \Omega$ for Fe/h-BN bilayer. The evolution of the resistance normalized against the bare resistance of Fe surface as a function of the number of h-BN layers on Fe is shown in Figure 1(d) and reveals an increase of approximately $10^{1.6} \Omega/\text{layer}$ of h-BN. The resistance increases exponentially as a function of the number of h-BN layers and falls within the range of the previous values obtained of similar experiments.^{16–18} A value of the h-BN barrier height of $\phi = 0.85 \text{ eV}$ is estimated from $\exp(-\sqrt{\phi}d) = 10^{-1.6}$ and $d = 0.4 \text{ nm}$ for the h-BN barrier thickness measured by AFM.⁷ The resistance CT-AFM mapping and the normalized resistance trend obtained confirm the homogeneous tunnel properties of our direct CVD h-BN layer over large areas. It also demonstrates the ability to control the tunnel barrier resistance with the number of layers, thanks to its intrinsic two-dimensional nature.

In Figure 2, we illustrate the device structure and present the transport characterization of the magnetic tunnel junctions using h-BN, directly grown by CVD, as a tunnel barrier and Fe and Co as ferromagnetic electrodes. In order to define the microjunctions (Figure 2(a)), we spincoat UVIII photoresist on the Fe/h-BN and subsequently pattern small openings of $30 \times 30 \mu\text{m}^2$ in the resist. Then, we deposit the Co (15 nm) ferromagnetic top electrode by evaporation on the whole sample and cap it with Au (80 nm). Finally, droplets of epoxy are deposited on the junctions to protect the Fe/h-BN/Co/Au structure and to act as a mask during a final ion beam etching step. I(V) and $dI/dV(V)$ spectroscopy characterization of the junction and magnetic transport measurements have been carried out with an AC-DC lock-in based measurement setup in a cryogenic measurement system at 1.4 K. The non-linear I(V) and parabolic $dI/dV(V)$ point to typical tunneling behavior (Figure 2(b)), validating our approach to integrate hBN directly by CVD in the MTJ device. No fine structure is seen in the parallel and antiparallel I(V) curves similarly to the case of amorphous Al₂O₃.

In Figure 3, we show the results of the magnetotransport measurements done with a 20 mV bias voltage at 1.4 K by switching the magnetization of the ferromagnetic electrodes. A TMR of $\sim 6\%$ is obtained (Figure 3(a)). The TMR value has been calculated by using the relation $TMR = \frac{R_{AP} - R_P}{R_P}$, where R_{AP} and R_P are the tunnel resistances measured in the antiparallel and parallel magnetization configurations of the ferromagnetic electrodes (based on the Jullière model^{21,27}). Additionally, we observe a decrease in the TMR with increasing voltage (Figure 3(b)), which is a typical behavior of

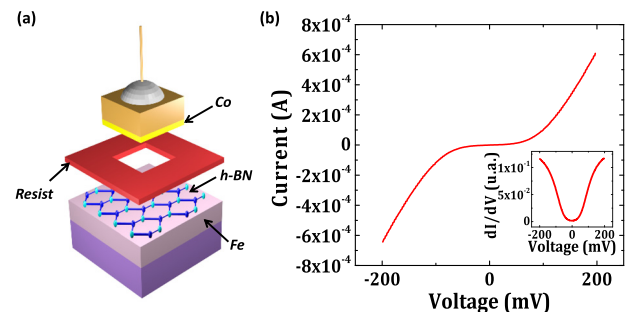


FIG. 2. (a) Schematic of the structure of a magnetic tunnel microjunction Fe/h-BN/Co. (b) I(V) and inset of $dI/dV(V)$ characterization of a Fe/h-BN/Co $30 \times 30 \mu\text{m}^2$ magnetic tunnel junction as a function of the voltage.

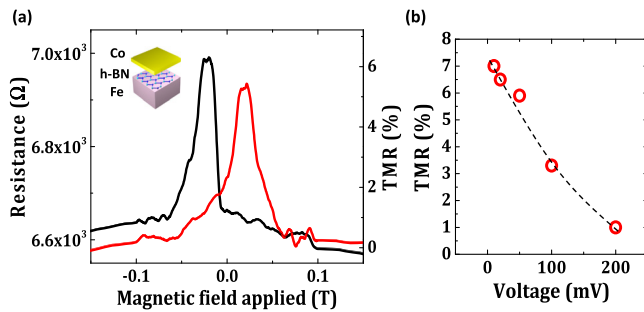


FIG. 3. (a) Tunnel magnetoresistance signal of $\sim 6\%$ measured on a Fe/h-BN/Co magnetic tunnel junction. (b) TMR behavior as the voltage is increased from 20 mV to 200 mV. The red dots are experimental data points whereas the dashed line is meant as a guide to the eye.

MTJs. With the measured value of TMR, we estimate the mean spin polarization P at the interfaces by using the relation $TMR = \frac{2P^2}{1-P^2}$, which gives a P value of $\sim 17\%$. While pioneering work by Dankert *et al.* reported values of 0.05% – 0.25% for the spin polarization in FM/h-BN/FM junctions,²⁰ our results are two orders of magnitude higher, highlighting the potential of h-BN as a tunnel barrier for spintronics. This vast improvement is certainly due to the direct CVD growth of the h-BN monolayer on the ferromagnetic metal, here Fe.

In conclusion, our results demonstrate the integration by direct CVD growth of atomically thin, homogeneous, and insulating h-BN tunnel barriers in magnetic tunnel junctions. The exponential dependence of the resistance as a function of the number of the h-BN layers clearly demonstrates the tunnel behavior of our h-BN layers on ferromagnets. The observed evolution falls within the results of other experiments.^{16–18} The possibility to multiply the barrier height and control it simply by adding other layers, thanks to CVD growth or the transfer method, is remarkable. Furthermore, the CT-AFM measurements show that the value of the resistance is constant over large regions of the sample, which is consistent with the fact that the tunnel behavior is homogeneous in the h-BN layer and that the direct CVD growth of h-BN on the ferromagnet is highly reliable. The $I(V)$ and $dI/dV(V)$ curves display the typical behavior of MTJs and the measured value of TMR of $\sim 6\%$ can be associated with a functional Fe/h-BN/Co microjunction. The values of the TMR and the spin polarization show a large improvement over previous experimental reports for MTJs using h-BN as a barrier.²⁰ While our result represents a large increase in the MR reported for the 2D materials based MTJs, we believe that many parameters remain open to exploration and improvement: dependence with the h-BN growth conditions, dependence with the underlying ferromagnets (Fe, Ni, Co, ... and alloys) and their crystallography, dependence with the epitaxy/rotation of h-BN. Our study is most certainly a demonstration which appeals deeper studies to get a better grasp on the underlying physics and target even larger MR. We believe that this result will lead to further investigations of the potential of h-BN (and other 2D materials or heterostructures) as tunnel barriers in MTJs.

S.C. acknowledges funding from EPSRC (Doctoral Training Award). R.S.W. acknowledges a Research

Fellowship from St. John's College, Cambridge and a Marie Skłodowska-Curie Individual Fellowship (Global) under grant ARTIST (no. 656870) from the European Union's Horizon 2020 research and innovation program. P.R.K. acknowledges a Lindemann Trust Fellowship. S.H. acknowledges funding from ERC grant InsituNANO (No. 279342) and EPSRC grant GRAPHTED (EP/K016636/1). P.S. acknowledges the Institut Universitaire de France for a junior fellowship. This research was partially supported by the EU FP7 Work Program under Grant GRAFOL (No. 285275) and Graphene Flagship (No. 604391), and by the Marie-Curie-ITN 607904-SPINOGRAPH.

- ¹C. Chappert, A. Fert, and F. N. Van Dau, *Nat. Mater.* **6**, 813 (2007).
- ²R. Wood, *J. Magn. Magn. Mater.* **321**, 555 (2009).
- ³A. V. Khvalkovskiy, D. Apalkov, S. Watts, R. Chepulskii, R. S. Beach, A. Ong, X. Tang, A. Driskill-Smith, W. H. Butler, and P. B. Visscher, *J. Phys. D: Appl. Phys.* **46**, 074001 (2013).
- ⁴A. Nagashima, N. Tejima, Y. Gamou, T. Kawai, and C. Oshima, *Phys. Rev. B* **51**, 4606 (1995).
- ⁵A. Varykhalov and O. Rader, *Phys. Rev. B* **80**, 035437 (2009).
- ⁶M.-B. Martin, B. Dlubak, R. S. Weatherup, M. Piquemal-Banci, H. Yang, R. Blume, R. Schloegl, S. Collin, F. Petroff, S. Hofmann, J. Robertson, A. Anane, A. Fert, and P. Seneor, *Appl. Phys. Lett.* **107**, 012408 (2015).
- ⁷S. Caneva, R. S. Weatherup, B. C. Bayer, B. Brennan, S. J. Spencer, K. Mingard, A. Cabrero-Vilatela, C. Baetz, A. J. Pollard, and S. Hofmann, *Nano Lett.* **15**, 1867 (2015).
- ⁸Y. S. Dedkov, M. Fomin, U. Rüdiger, and C. Laubschat, *Appl. Phys. Lett.* **93**, 022509 (2008).
- ⁹N. Rougemaille, A. N'Diaye, J. Coraux, C. Vo-Van, O. Fruchart, and A. K. Schmid, *Appl. Phys. Lett.* **101**, 142403 (2012).
- ¹⁰O. V. Yazyev and A. Pasquarello, *Phys. Rev. B* **80**, 035408 (2009).
- ¹¹V. M. Karpan, P. A. Khomyakov, G. Giovannetti, A. A. Starikov, and P. J. Kelly, *Phys. Rev. B* **84**, 153406 (2011).
- ¹²C. R. Dean, A. F. Young, I. Meric, C. Lee, L. Wang, S. Sorgenfrei, K. Watanabe, T. Taniguchi, P. Kim, K. L. Shepard, and J. Hone, *Nat. Nanotechnol.* **5**, 722 (2010).
- ¹³T. Yamaguchi, Y. Inoue, S. Masubuchi, S. Morikawa, M. Onuki, K. Watanabe, T. Taniguchi, R. Moriya, and T. Machida, *Appl. Phys. Express* **6**, 073001 (2013).
- ¹⁴M. Yankowitz, J. Xue, and B. J. LeRoy, *J. Phys.: Condens. Matter* **26**, 303201 (2014).
- ¹⁵A. K. Geim and I. V. Grigorieva, *Nature* **499**, 419 (2013).
- ¹⁶G.-H. Lee, Y.-J. Yu, C. Lee, C. Dean, K. L. Shepard, P. Kim, and J. Hone, *Appl. Phys. Lett.* **99**, 243114 (2011).
- ¹⁷L. Britnell, R. V. Gorbachev, R. Jalil, B. D. Belle, F. Schedin, M. I. Katsnelson, L. Eaves, S. V. Morozov, A. S. Mayorov, N. M. R. Peres, A. H. Castro Neto, J. Leist, A. K. Geim, L. A. Ponomarenko, and K. S. Novoselov, *Nano Lett.* **12**, 1707 (2012).
- ¹⁸M. V. Kamalakar, A. Dankert, J. Bergsten, T. Ive, and S. P. Dash, *Sci. Rep.* **4**, 6146 (2014).
- ¹⁹M. L. Hu, Y. Zhizhou, K. W. Zhang, L. Z. Sun, and J. X. Zhong, *J. Phys. Chem. C* **115**, 8260 (2011).
- ²⁰A. Dankert, M. V. Kamalakar, A. Wajid, R. S. Patel, and S. P. Dash, *Nano Res.* **8**, 1357 (2015).
- ²¹M. Jullière, *Phys. Lett. A* **54**, 225 (1975).
- ²²A. Olbrich, B. Ebersberger, and C. Boit, *Appl. Phys. Lett.* **73**, 3114 (1998).
- ²³A. Ando, R. Hasunuma, T. Maeda, K. Sakamoto, K. Miki, Y. Nishioka, and T. Sakamoto, *Appl. Surf. Sci.* **162**, 401 (2000).
- ²⁴B. Dlubak, M.-B. Martin, C. Deranlot, K. Bouzehouane, S. Fusil, R. Mattana, F. Petroff, A. Anane, P. Seneor, and A. Fert, *Appl. Phys. Lett.* **101**, 203104 (2012).
- ²⁵J. Y. Park, Y. Qi, P. D. Ashby, L. M. Hendriksen, and M. Salmeron, *J. Chem. Phys.* **130**, 114705 (2009).
- ²⁶P. R. Kidambi, R. Blume, J. Kling, J. B. Wagner, C. Baetz, R. S. Weatherup, R. Schloegl, B. C. Bayer, and S. Hofmann, *Chem. Mater.* **26**, 6380 (2014).
- ²⁷J. M. MacLaren, X.-G. Zhang, and W. H. Butler, *Phys. Rev. B* **56**, 11827 (1997).